Penerbit Akademia Baru

Journal of Advanced Research in Micro and Nano Engineering

Journal homepage: https://akademiabaru.com/submit/index.php/armne
ISSN: 2756-8210

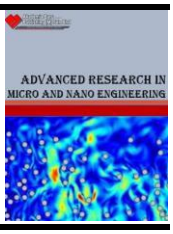

Effects of Solar Radiation and Viscous Dissipation on Mixed Convective Non-Isothermal Hybrid Nanofluid over Moving Thin Needle

Sultana Jahan[1], M. Ferdows[1,*], MD Shamshuddin[2], Khairy Zaimi[3]

[1] Research Group of Fluid Flow Modelling and Simulation, Department of Applied Mathematics, University of Dhaka, Dhaka-1000, Bangladesh
[2] Department of Mathematics, Vaagdevi College of Engineering (Autonomous), Warangal, Telangana, India
[3] Institute of Engineering Mathematics, Universiti Malaysia Perlis, Pauh Putra Campus, 02600 Arau, Perlis, Malaysia

ABSTRACT

The article is to examine the simulations influence of exponential solar radiation and dissipative transport of steady mixed convective hybrid nanofluid flow regime for an incompressible fluid in the boundary layer limit past a non-isothermal moving thin needle. We solved the system of ordinary differential equations obtained by choosing appropriate non-dimensional variables using the MAPLE software scheme. We have discussed the flow behaviours and all physical quantities of interest like skin friction cofactor, rate of heat transfer and rate of mass transfer as a function of similarity variables and governing parameters. Our numerically calculated solutions are given with similar studies. For instance, the entrance of several parameters like mixed convection, Power Law constant, buoyancy ratio parameter, Eckert number are illustrated graphically on velocity, temperature and nanoparticle concentration profiles. We observed that, the rate of heat transfer is higher in all cases but the reduction of mass transfer rate has been noticed.

Keywords:
Boundary layer flow; Mixed convection;
solar radiation; Non-Isothermal;
Viscous dissipation; Moving thin
Needle; Hybrid nanofluid

Received: 21 Dec. 2020 **Revised: 8 Feb. 2021** **Accepted: 3 Mar. 2021** **Published: 22 Mar. 2021**

1. Introduction

Boundary layer flow [1] and heat transfer are the fundamental areas of the modern fluid dynamics, which have huge application in engineering and industrial fields. Boundary layer is the region, where viscosity is dominant and the majority of the drag experienced by the body immersed in a fluid is created, the viscosity can be neglected on the outside of the boundary layer without any significant effects. It has several application including polymer extrusions, wire drawing, nuclear reactor etc. are the examples of such flow in engineering and industrial processes.

The analysis of heat transfer and boundary layer flow has gathered an immense attention from researchers which focused on hybrid nanofluid, in recent period. Hybrid nanofluid has more thermophysical properties [2] and it has the capacity of raising the heat transfer rate because of the

* *Corresponding author.*
E-mail address: ferdows@du.ac.bd

synergistic effects [3]. Better understanding of thermal capacity of hybrid nanofluid in comparison with nanofluid has been analysed [4]. Hybrid nanofluid is considered as an effective heat transfer fluid rather than nanofluid and base fluid which uses for engineering application, to augment the heat transfer in the system [5]. It also has phenomenal application in the branches of heat exchanger, nuclear system cooling, coolant in machining, transformer cooling, solar collector, micro power generation, heat sink, boiling, electronic cooling, refrigeration, drug reduction, biomedical [6]. With transpiration effect [7] dual solution is noticed for both shrinking and stretching sheet, using buoyancy effect [8] bifurcation is found which lead the solution towards a lower point. Though dual solution has been found [9] for several value of radiation and suction parameter, skin fraction factor decreased for first solution. Dual solution is also noticeable for unsteadiness parameter [10]. For the elevated value of volume fraction of nanoparticle, critical value decreased in biaxial sheet [11]. With the wide range of Reynolds number, it is noticed that the heat transfer rate and skin friction coefficients got higher in stretching/shrinking cylinder [12].

Over the last decades the problem of boundary layer flow past thin needle [13] has been proven as beneficial in terms of applications specially in industrial areas, for example electronic devices, the hot wire anemometer, geothermal power generation. It has also some vital aspects in the industries of engineering and medicine such as lubrication, blood flow problems, manufacturing dynamics of smart coating, wind prediction, transportation etc. [14]. Forced convection boundary layer flow through a horizontal thin needle [15] has been initiated which showed that the fluid and hear transfer was affected by solid volume fraction. For further assumption [16] another problem examined on the velocity and temperature profiles with a visible impact of needle size as well as solid volume fraction. Laminar mixed convective flow of hybrid nanofluid is investigated for experimental learning [17,18]. Vertical thin needle with mixed convection boundary layer flow were obtained to find out the effect of solid volume fraction and boundary layer separation [19].

To our best knowledge, no study has taken place in order to examine an incompressible hybrid nanofluid in the boundary layer with the influence of exponential solar radiation [20,21] and viscous dissipation [22] of steady mixed convective heat transfer flow past a non-isothermal moving thin needle. Here we consider ($Al_2O_3 - Cu - water$) as a hybrid nanofluid and the effects of Brownian motion and thermophoresis [23] are included in this paper for this fluid.

2. Physical Model and Formulation

Study of a solar radiative dissipative, inspired by simulating the functional mixed convective hybrid nano-polymer coating boundary layer flow on a moving thin needle containing different nanoparticles. Temperature variation as $T = T_w = T_\infty + Ax^P$ considered for the condition of non-isothermal case, with surface temperature T_w and the ambient temperature T_∞ ($T_w > T_\infty$). The adopted cylindrical coordinate system (x, r) (Figure 1) with axial (x) and radial (r) coordinates, respectively. Here the needle moves with a constant speed U_∞ in a moving fluid with the same speed, C_w is the nanoparticle concentration at surface and C_∞ is the ambient nanoparticle concentration. The properties of nanofluid are assumed to be constant. The corresponding governing equations, under above assumptions describing the 2D Hybrid nanofluid boundary layer flow is obtained by amalgamating earlier models ([20],[22],[23]).

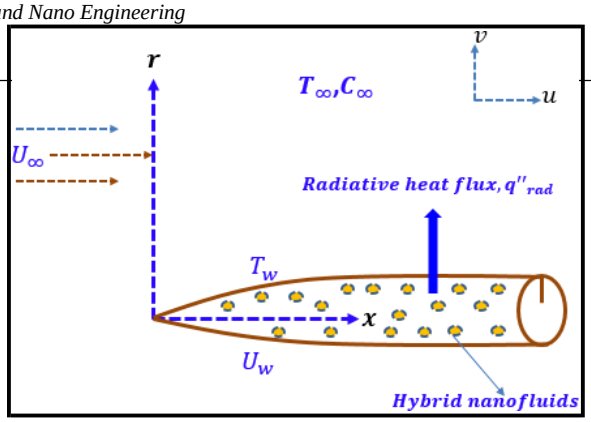

Fig. 1. Flow geometry of hybrid nanofluid through thin needle

$$\frac{\partial}{\partial x}(ru) + \frac{\partial}{\partial r}(rv) = 0 \tag{1}$$

$$u\frac{\partial u}{\partial x} + v\frac{\partial u}{\partial r} = \frac{\mu_{hnf}}{\rho_{hnf}}\frac{1}{r}\frac{\partial}{\partial r}\left(r\frac{\partial u}{\partial r}\right) + \frac{1}{\rho_f}[(1-C_\infty)\rho_{f\infty}\beta(T - T_\infty) - (\rho_p - \rho_{f\infty})(C - C_\infty)]g \tag{2}$$

$$u\frac{\partial T}{\partial x} + v\frac{\partial T}{\partial r} = \frac{1}{r}\frac{\kappa_{hnf}}{(\rho C_p)_{hnf}}\frac{\partial}{\partial r}\left(r\frac{\partial T}{\partial r}\right) + \sigma\left[D_B\frac{\partial C}{\partial r}\frac{\partial T}{\partial r} + \frac{D_T}{T_\infty}\left(\frac{\partial T}{\partial r}\right)^2\right] + \frac{1}{(\rho C_p)_{hnf}}\frac{\partial q''_{rad}}{\partial r} + \frac{\mu_{hnf}}{(C_p)_{hnf}}\left(\frac{\partial u}{\partial r}\right)^2 \tag{3}$$

$$u\frac{\partial C}{\partial x} + v\frac{\partial C}{\partial r} = \frac{D_B}{r}\frac{\partial}{\partial r}\left(r\frac{\partial C}{\partial r}\right) + \frac{D_T}{T_\infty}\frac{1}{r}\frac{\partial}{\partial r}\left(r\frac{\partial T}{\partial r}\right) \tag{4}$$

Boundary conditions for the flow geometry are:

$$u = U_\infty\varepsilon,\ \ v = v_w,\ \ T = T_w = T_\infty + Ax^P,\ \ D_B\frac{\partial C}{\partial r} + \frac{D_T}{T_\infty}\frac{\partial T}{\partial r} = 0 \text{ at } r = R(x)$$

$$u \to U_\infty,\ T \to T_\infty,\ C \to C_\infty \text{ as } r \to \infty \tag{5}$$

where, A, p are constant, ε is constant moving parameter, u and v are the velocity components in (x, r) directions, the surface of the thin needle is described by R(x), D_T and D_B are thermophoretic diffusion and Brownian diffusion coefficients, respectively, the effective heat capacity ratio, hybrid nanofluid's temperature, nanoparticle concentration and mass flux velocity are represented with $\boldsymbol{\sigma}$,T, C and v_w respectively, heat capacity, thermal conductivity, dynamic viscosity and density of hybrid nanofluid flow are characterized by $(\rho C_p)_{hnf}$,k_{hnf}, μ_{hnf} and ρ_{hnf} respectively. Further, the nanoparticle volume fractions of Al_2O_3 *and* Cu are symbolised by φ_1*and* φ_2 while their solid components are indicated by the subscripts n1 and n2, respectively. Thermophysical properties are listed in Table-1.

Table 1
Thermophysical properties of nanoparticles and water (see [14, 23])

Thermophysical properties	water	Cu	Al_2O_3
ρ	997.1	8933	3970
C_p	4179	385	765
k	0.613	400	40

Eq. (1-5) are formidable to solve even with numerical methods. It is pertinent therefore to simplify them with the help of similarity transformations and dimensionless quantities assuming from ([12-13])

$$\psi = \nu_f x\, f(\eta),\ \theta(\eta) = \frac{T - T_\infty}{T_W - T_\infty},\ \varphi(\eta) = \frac{C - C_\infty}{C_\infty},\ \eta = \frac{U_\infty r^2}{\nu_f x},\ q''_{rad} = 1 - \exp(-a_1 r),\ R(x) = \left(\frac{\nu_f c x}{U_\infty}\right)^{\frac{1}{2}} \quad (6)$$

Using (6), Eq. (2) to (5) become

$$2\frac{c1}{c2}(\eta f'')' + ff'' + \frac{\xi\theta}{4} - \frac{Nr\phi}{4} = 0 \quad (7)$$

$$\frac{1}{Pr}\frac{c4}{c3}(\eta\theta')' + \frac{1}{2}f\theta' - \frac{1}{2}Pf'\theta + \eta[Nb\phi'\theta' + Nt\theta'^2] +$$

$$\frac{c1}{c3}\,4Ec\eta f''^2 + \frac{Ga}{2}\,c5\exp\left(-a\eta^{\frac{1}{2}}Re^{\frac{-1}{2}}\right) = 0 \quad (8)$$

$$2(\eta\varphi')' + Scf\phi' + 2\frac{Nt}{Nb}(\eta\theta')' = 0 \quad (9)$$

Subjected to

$$f(c) = \varepsilon c,\ f'(c) = \frac{\varepsilon}{2},\ \theta(c) = 1,\ Nb\phi'(c) + Nt\theta'(c) = 0$$

$$f'(\eta) \to \frac{1}{2},\ \theta(\eta) \to 0,\ \phi(\eta) \to 0 \text{ as } \eta \to \infty \quad (10)$$

where, Ec, ξ, Gr_x, Re, ε, Nr, Pr, Sc, Nt, Nb signifies respectively Eckert number, local Grashof number, Reynolds number, constant moving parameter, buoyancy ratio parameter, Prandtl number, Schmidt number, thermophoresis and Brownian motion parameters, respectively. The needle moves away from the origin if ε > 0 and moves toward the origin if ε < 0. The dimensionless flow parameters arising in Eq. (7-10) have the following mathematical definitions:

$$Pr = \frac{\nu_f(\rho c_p)_f}{k_f},\ Sc = \frac{\nu_f}{D_B},\ Nt = \frac{\sigma D_T(T_W - T_\infty)}{\nu_f T_\infty},\ Ec = \frac{U_\infty^2}{c_p(T_W - T_\infty)},\ \xi = \frac{Gr_x}{Re^2} = \frac{(1-C_\infty)(T-T_\infty)g\rho_f\beta x}{U_\infty^2\rho_f},$$
$$Nr = \frac{(C-C_\infty)(\rho_p - \rho_{f\infty})gx}{U_\infty^2\rho_f},\ Nb = \frac{\sigma D_B C_\infty}{\nu_f},\ Ga = \frac{axq''_{rad}}{(T-T_\infty)2U_\infty},\ c1 = \frac{\mu_{hnf}}{\mu_f} = \frac{1}{(1-\varphi_1)^{2.5}(1-\varphi_2)^{2.5}}$$
$$c2 = \frac{\rho_{hnf}}{\rho_f} = \frac{(1-\varphi_2)[(1-\varphi_1)\rho_f + \varphi_1\rho_{n1}] + \varphi_2\rho_{n2}}{\rho_f},\ c3 = \frac{(\rho C_p)_{hnf}}{(\rho C_p)_f} = \frac{(1-\varphi_2)[(1-\varphi_1)(\rho C_p)_f + \varphi_1(\rho C_p)_{n1}] + \varphi_2(\rho C_p)_{n2}}{(\rho C_p)_f}$$
$$c4 = \frac{k_{hnf}}{k_{nf}},\ \frac{k_{hnf}}{k_f} = \frac{k_{n2} + 2\varphi_2 k_{n2} + k_{nf}(2 - 2\varphi_2)}{k_{n2} - \varphi_2 k_{n2} + k_{nf}(2 + \varphi_2)}\ where,\ \frac{k_{nf}}{k_f} = \left(\frac{k_{n1} + 2k_f - 2\varphi_1(k_f - k_{n1})}{k_{n1} + 2k_f + \varphi_1(k_f - k_{n1})}\right)$$
$$c5 = \frac{1}{(\rho C_p)_{hnf}} = \frac{1}{(1-\varphi_2)[(1-\varphi_1)(\rho C_p)_f + \varphi_1(\rho C_p)_{n1}] + \varphi_2(\rho C_p)_{n2}} \quad (11)$$

Local skin friction coefficient C_f, Nusselt number Nu_x and Sherwood numbers Sh_x are given by

$$Re_x^{\frac{1}{2}}C_f = 4c^{\frac{1}{2}}\frac{\mu_{hnf}}{\mu_f}f''(0),\ Re_x^{-\frac{1}{2}}Nu_x = -2c^{\frac{1}{2}}\frac{k_{hnf}}{k_f}\theta'(c),$$
$$Re_x^{\frac{-1}{2}}Sh_x = -2c^{\frac{1}{2}}\phi'(c) = 2c^{\frac{1}{2}}\frac{Nt}{Nb}\theta'(c) \quad (12)$$

3. Numerical Procedure and Result Discussion

Numerical investigation of a mixed convective steady non-isothermal hybrid nanofluid flow moving thin needle containing different nanoparticles is studied extensively. Extensive numerical MAPLE software scheme computations that can accommodate complex boundary conditions (10) and multiple nonlinear coupled boundary layer Eq. (7-9) have been performed and all results are visualised in Figs 2-16. Once the velocity, temperature and nanoparticle concentration variables are evaluated, the skin friction, Nusselt number and Sherwood number may be readily computed, compared with previously published results and documented in Table 2-3. Further, the computed results of Skin friction, Nusselt number and Sherwood number for the other parameters are presented in Table 4. To validate the present numerical results, we consider various volume fraction φ_2 of Cu, while the volume fraction φ_1 = 0.1 of Al_2O_3 is kept fixed. The values of f''(c) and -θ'(c) when ϕ_1=ϕ_2=0 (regular fluid), $\varepsilon = Sc = 0$ and $Pr = 0.7$ for various values of c in the absence of Nt and Nb are displayed in Table 2 and found good accuracy to run further simulations [14, 23]. On the other hand, Table 3 is provided to describe the values of f''(c) and -θ'(c) for Cu-water nanofluid when $\varphi_1 = \varepsilon = Sc = 0$ and $Pr = 7$ with various values of c and φ_2 in the absence of Nt and Nb. The present numerical results are compared with the previous results obtained [23] and show a favourable agreement. For less the needle size, the enhancement of f''(c) and -θ'(c) can be observed from Table 2 to 4 and it was observed that φ_2 tend to increase the values of f''(c) and but decrease the values of -θ'(c) as $\varphi_2$increases. MAPLE software scheme and this method was used by several researchers, for instance, [24,25] to calculate their results more accurately.

Table 2
Values of $f''(c)$ and -$\theta'(c)$ for $\varphi_1 = \varphi_2 = 0$, $\varepsilon = Sc = 0$, Pr = 0.733 with the value of c

c	Grosan and Pop [14] $f''(c)$	Waini, Ishak and pop [23] $f''(c)$	Present work $f''(c)$	Grosan and Pop [14] -$\theta'(c)$	Present work -$\theta'(c)$
0.1	1.289074	1.288778	1.317999	2.441675	2.535714

Table 3
Values of $f''(c)$ and -$\theta'(c)$ for regular fluid ($\varphi_1 = \varphi_2 = 0$) when ($\varepsilon = Sc = 0$) and $Pr = 7$ with the various values of c and φ_2, where Nb and Nt are absent

		$f''(c)$		$-\theta'(c)$	
c	φ_2	Waini, Ishak and Pop [23]	Present work	Waini, Ishak and Pop [23]	Present work
0.1	0.05 0.1 0.2	1.347125 1.381635 1.404050	1.365640 1.394255 1.413123	3.681817 3.586427 3.389682	3.688617 3.588975 3.389044

Figure 2-4 exhibit the disparity of velocity, temperature and concentration sketches through dissimilar quantities of mixed convection parameter ξ, where $Pr = 6.2$, $Nr = 0.1$, $P = 1$, $Ec = 0.1$, $Ga = 1.25$, $Sc = 0.5$, $\phi_1 = 0.1$, $a = 6$, $Re = 1$, $\phi_2 = 0.1$, $c = 0.1$, $\varepsilon = -1$. The velocity reports magnify through an escalating in mixed convection quantity for both the nanoparticles considered, the elucidations of that performance reveal that the momentum boundary layer growth is accelerated the fluid motion. On the other hand, temperature reports lessen through an escalating in mixed convection quantity in the whole liquid region. Further, an improvement in the mixed convection quantity enhances concentration results rapidly, asymptotically satisfy the free stream conditions (10).

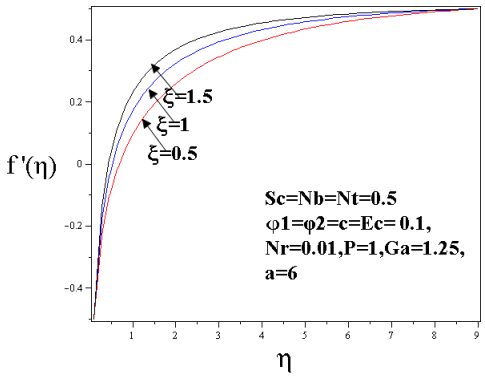

Fig:2 Impact of ξ on f '(η)

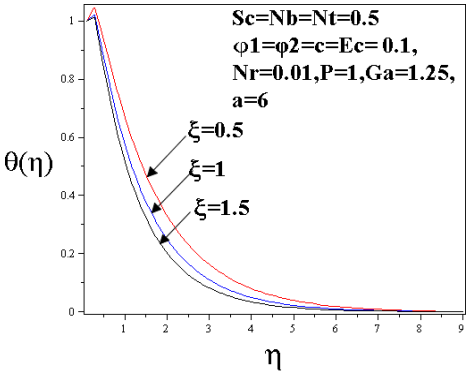

Fig 3: Impact of ξ on θ(η)

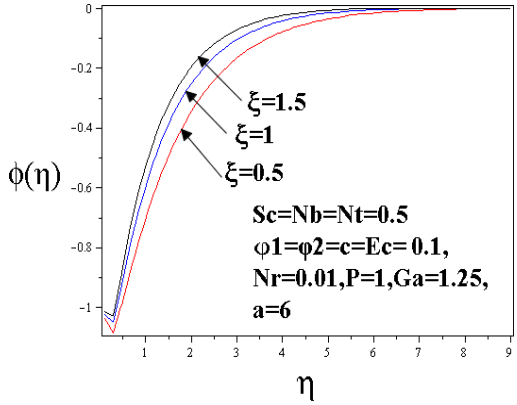

Fig:4 Impact of ξ on ϕ(η)

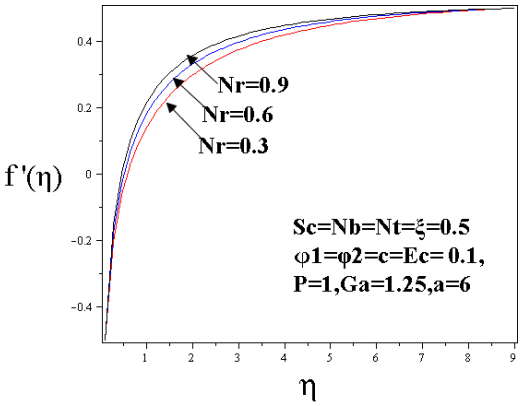

Fig 5: Impact of Nr on f '(η)

Figure 5-7 discloses the consequences of solutal buoyancy parameter Nr, on the liquid velocity, temperature and concentration constituents. The velocity improved by an increasing in solutal buoyancy parameter Nr, all over the liquid section. Generally, concentration buoyancy parameter appears in the momentum equation, the thermal Grashof quantity Gr, implies qualified outcome of the heat buoyancies strength for the glutinous hydrodynamic vigour during the edge stratum, near the same time, as the mass Grashof's quantity Gm, established the ratio for the concentration buoyancies strength to the glutinous hydrodynamic vigor. As accepted the nanoliquid rapidly increases by asset of the intensification of solutal buoyancy's service. The rapidity delivery increases speedily next to the thin needle afterwards, those in turn downs effortlessly for the gratuitous stream number. Hence, frontier layers width enlarges through boost uo in solutal buoyancy parameter. i.e. the improvement Nr prepared the liquid movement upsurges for temperature. Therefore, the resulting temperature was enhanced by an augment in concentration buoyancy parameter. Further, an improvement in the concentration buoyancy parameter reduces the concentration result rapidly.

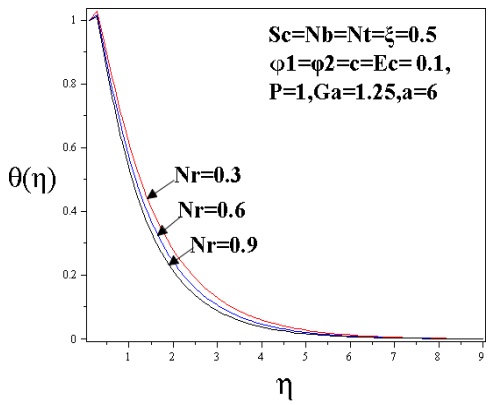

Fig 6: Impact of Nr on θ(η)

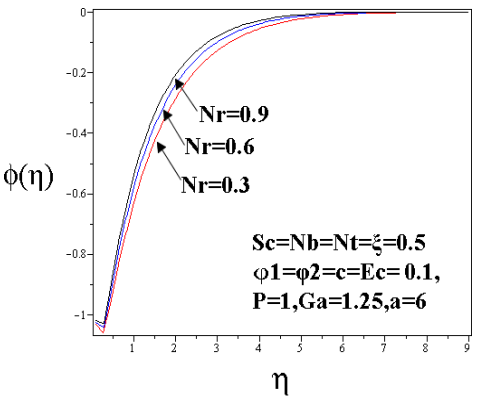

Fig 7: Impact of Nr on f '(η)

Figure 8-10 visualise the response in radial velocity, temperature and concentration distributions with power law constant P. $P = 0$ corresponds to uniform surface temperature, $P = 1/3$ corresponds to uniform surface heat flux and $P = 1$ corresponds to isothermal surface. As seen, radial flow rate profiles diminish due to rising power law constant that resulted in rising nanofluid bonding strength. As power law constant appeared in boundary condition (5) depending on indexing, which diminishes the viscous force due to radial flow. However, the opposite in the heat distribution responses is noticed due to strong resistance to the heat generated. A more significant increment is computed throughout the concentration liquid region with rise in power law constant.

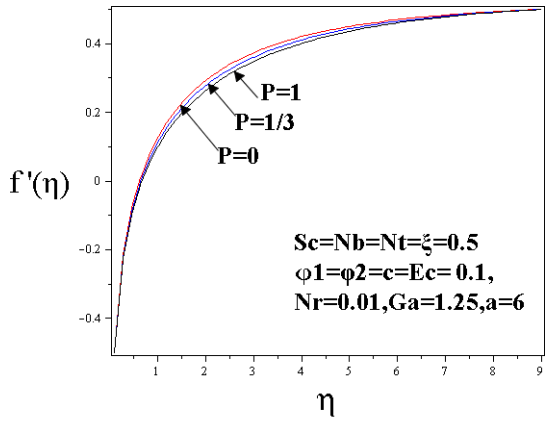

Fig 8: Impact of P on f '(η)

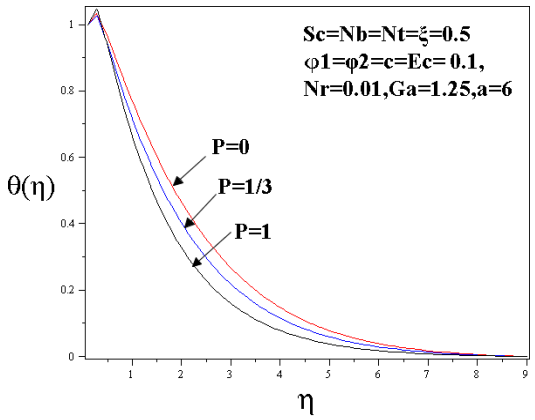

Fig 9: Impact of P on θ(η)

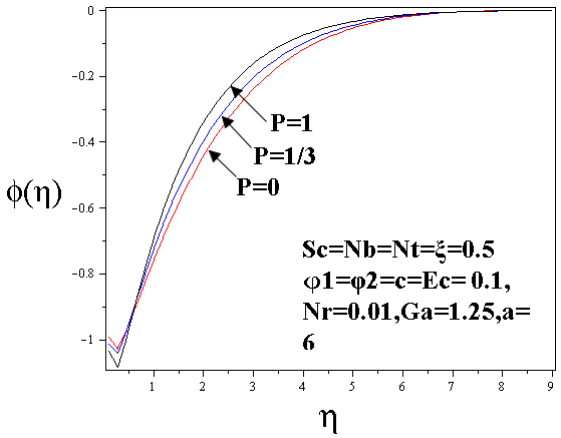

Fig 10: Impact of P on ϕ(η)

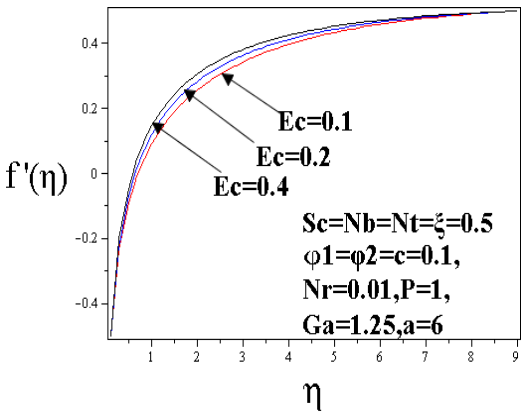

Fig 11: Impact of Ec on f '(η)

Figure 11-13 illustrates the distributions in velocity, temperature and concentration with Eckert number, Ec. Eckert number expresses the relative contribution of kinetic energy in the nanopolymer flow to the boundary layer enthalpy difference. It features in viscous (mechanical) heating equation. Even relatively small values of Ec exert a significant influence on thermal field. Also, Eckert number acts an appreciated part in the description of continuum mechanics. Notable enhancement is induced in radial flow rate. An increase in Eckert number is observed to strongly elevate temperatures throughout the boundary layer regime, irrespective of the nanoparticle considered. There is increasing conversion of kinetic energy in the boundary layer flow to thermal energy owing to internal friction with higher Eckert numbers. Hence, thermal boundary layer thickness is therefore also enhanced with dissipation effect. However, a strong depletion in nanoparticle concentration magnitudes is observed with rise in Eckert number. Asymptotically smooth solutions are achieved in the free stream confirming the prescription of an adequately large infinity boundary condition in the MAPLE quadrature code.

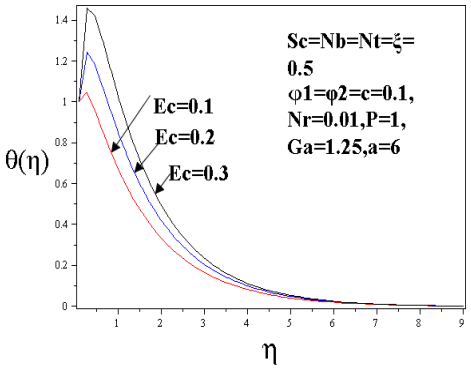

Fig 12: Impact of Ec on θ(η)

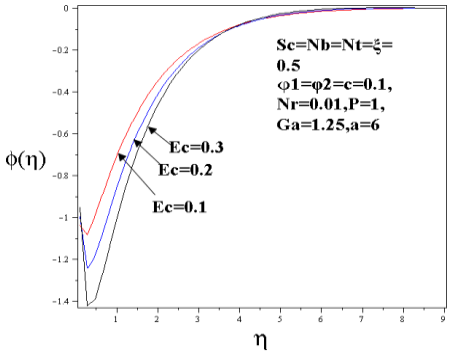

Fig 13: Impact of Ec on ϕ(η)

Figure 14-16 shows the evolution in $f'(\eta)$, $\theta(\eta)$, $\phi(\eta)$ profiles for different nanoparticles with transverse coordinate to a modification in nanoparticle volume fraction ϕ_2. It is evident that a strong declination in the flow is generated with higher fractional volume of nanoparticles i.e. the thickness of the hydrodynamic boundary layer reduces. It is apparent from Figure 15 that a strong accentuation in temperature is mobilised with higher nanoparticle volume fractions i.e. greater doping percentage of the base fluid. Therefore, thickness of thermal boundary layer increases. The flow distribution indeed confirms the non-trivial effect of nanoparticle doping as a strong mechanism for elevating both convection and conduction coefficients. Hence, nanofluids are effective for energizing base fluids without the clogging effects encountered with micro-scaled particles. They increase thermal efficiency of process and these are beneficial n coating dynamics since extra mechanism is available for regulating heat transfer effects and more precisely manipulating finishing characteristics. However, a strong depletion in nanoparticle concentration magnitudes is observed with rise in volume fraction.

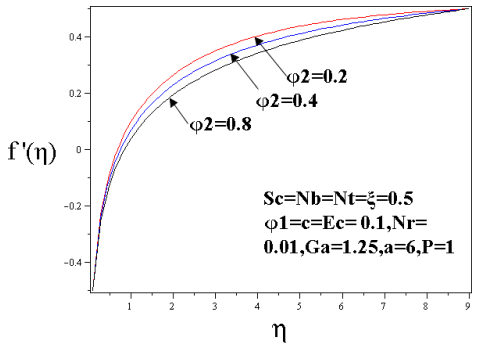

Fig 14: Impact of φ_2 on f '(η)

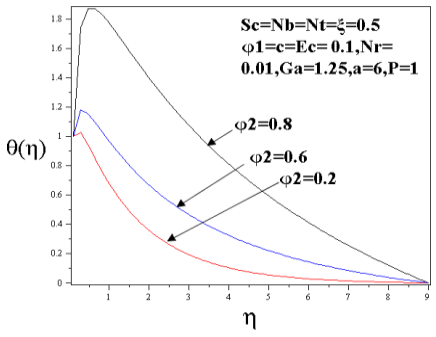

Fig 15: Impact of φ_2 on θ(η)

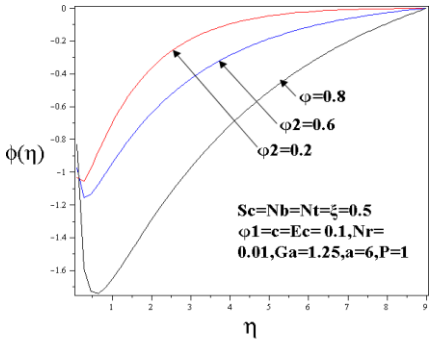

Fig 16: Impact of φ_2 on ϕ(η)

Table 4 show that with enhancing ϕ_2, ξ, P, Nr and Ec trends are as follows; with increasing volume fraction ϕ_2, skin friction, $f''(\eta)$ and Sherwood number, $\phi'(\eta)$ are reduced whereas Nusselt number $\theta'(\eta)$ is elevated. With greater mixed convection parameter ξ, skin friction and Nusselt number are elevated and Sherwood number is reduced. With greater power law constant P, skin friction and Sherwood number are reduced whereas Nusselt number is elevated. With increase in solutal buoyancy parameter Nr, skin friction and Nusselt number are strongly elevated but reduces the Sherwood number. Finally, Grater Ec values decrease Sherwood number but increase skin friction and Nusselt number.

Table 4
Skin friction coefficient, Nusselt number and Sherwood numbers and the values of other parameter is Pr = 6.2, Ga =1.25, Sc = 0.5, φ_1= 0.1, a = 6, Re = 1, c=0.1, $\varepsilon = -1$, Nb = 0.5, Nt = 0.5.

φ_2	ξ	P	Nr	Ec	$f''(\eta)$	$\theta'(\eta)$	$\phi'(\eta)$
0.2 0.6 0.8	0.5	1	0.01	0.1	2.5525 2.4685 2.3490	1.4556 3.2430 10.2467	-1.4556 -3.2430 -10.2467
0.1	0.5 1 1.5	1	0.01	0.1	2.5873 3.1042 3.5493	1.7697 1.8691 2.1000	-1.7697 -1.8691 -2.1000
0.1	0.5	0 $\frac{1}{3}$ 1	0.01	0.1	2.7248 2.6391 2.6110	1.2201 1.2649 1.7691	-1.2201 -1.2649 -1.7691
0.1	0.5	1	0.3 0.6 0.9	0.1	2.8474 3.1304 3.3867	1.7204 1.8035 1.9206	-1.7204 -1.8035 -1.9206
0.1	0.5	1	0.01	0.1 0.2 0.3	2.5344 2.6866 2.8353	1.6994 4.4117 7.4979	-1.6994 -4.4117 -7.4979

4. Conclusions

MAPLE software scheme numerical solutions have been derived for incompressible mixed convection non-isothermal hybrid nanofluid transport through moving thin needle with the impacts of solar thermal radiation and viscous dissipation. Two different water based nanofluids have been examined, of relevance to smart functional nano-polymers. Graphical results for velocity, temperature and nanoparticle concentration distributions have been presented for different parametric cases. Skin friction, Nusselt number and Sherwood number distributions have also been computed. Key observation of the outcomes reveals that enhancement in ξ, Nr accelerates the boundary layer flow (thinner momentum boundary layer) whereas elevation in Eckert number

induces a deceleration (thicker momentum boundary layer). Increasing Eckert number elevates temperature strongly but suppresses the nanoparticle concentration magnitudes. Higher mixed convection parameter, solutal buoyancy parameter and Eckert numbers significantly elevates skin friction and Nusselt number but weekly reduces for Sherwood number.

References

[1] L. Prandtl, U¨ ber Flu¨ ssigkeitsbewegungen bei sehr kleiner Reibung, Verhandlg. III Intern. Math. Kongr. Heidelberg. ,484– 491, 1904.

[2] L. Syam Sundara, K.V. Sharmab, Manoj K. Singha, A.C.M. Sousa, "Hybrid nanofluids preparation, thermal properties, heat transfer and friction factor – A review", Renewable and Sustainable Energy Reviews, 68, 185-198, 2017. https://doi.org/10.1016/j.rser.2016.09.108

[3] Jahar Sarkar, Pradyumna Ghosh, Arjumand Adil, "A review on hybrid nanofluids: Recent research, development and applications", Renewable and Sustainable Energy Reviews, 43, 164-177, 2015.https://doi.org/10.1016/j.rser.2014.11.023 .

[4] Hemmat Esfe, M.; Alirezaie, A.; Rejvani, M. "An applicable study on the thermal conductivity of SWCNT-MgO hybrid nanofluid and price-performance analysis for energy management." Appl. Therm. Eng. 111,1202–1210, 2017. http://dx.doi.org/10.1016/j.applthermaleng.2016.09.091

[5] Waini, I.; Ishak, A.; Pop, I., "Flow and heat transfer of ahybrid nanafluid past a permeable moving surface", Chinese Journal of Physics, 66, 606-619, 2020. https://doi.org/10.1016/j.cjph.2020.04.024

[6] Umair Khan; Anum Shafiq; A. Zaib; Dumitru Baleanu, "Hybrid nanofluid on mixed convective radiative flow from an irregular variably thick moving surface with convex and concave effects", Case Studies in Thermal Engineering, 21, 2020. https://doi.org/10.1016/j.csite.2020.100660

[7] Waini, I., Ishak, A. and Pop, I, "Transpiration effects on hybrid nanofluid flow and heat transfer over a stretching/shrinking sheet with uniform shear flow", Alexandria Engineering Journal, 59, 91-99, 2020. https://doi.org/10.1016/j.aej.2019.12.010

[8] Waini, I., Ishak, A. and Pop, I., "Hybrid nanofluid flow towards a stagnation point on an exponentially stretching/shrinking vertical sheet with buoyancy effects", International Journal of Numerical Methods for Heat & Fluid Flow,30, 2020. https://doi.org/10.1108/HFF-02-2020-0086

[9] Yashkun, U., Zaimi, K., Abu Bakar, N.A., Ishak, A. and Pop, I. "MHD hybrid nanofluid flow over a permeable stretching/shrinking sheet with thermal radiation effect", International Journal of Numerical Methods for Heat & Fluid Flow, 10, 2020. https://doi.org/10.1108/HFF-02-2020-0083

[10] Iskandar Waini, Anuar Ishak, Ioan Pop, "Unsteady flow and heat transfer past a stretching/shrinking sheet in a hybrid nanofluid", International Journal of Heat and Mass Transfer, 136, 288-297, 2019. https://doi.org/10.1016/j.ijheatmasstransfer.2019.02.101

[11] Waini, I., Ishak, A. and Pop, I., "Hybrid nanofluid flow and heat transfer over a permeable biaxial stretching/shrinking sheet", International Journal of Numerical Methods for Heat & Fluid Flow, 30, 3497-3513, 2019. https://doi.org/10.1108/HFF-07-2019-0557

[12] Iskandar Waini, Anuar Ishak & Ioan Pop, "Hybrid nanofluid flow towards a stagnation point on a stretching/shrinking cylinder", Scientific Reports, 10, 2020. https://doi.org/10.1038/s41598-020-66126-2

[13] Lee, L.L, "Boundary layer over a thin needle". Phys. Fluids,10,820–822,1967. https://doi.org/10.1063/1.1762194

[14] I Waini, A Ishak, I Pop, "Hybrid nanofluid flow and heat transfer past a vertical thin needle with prescribed surface heat flux". Int. J. Numer. Methods Heat Fluid Flow, 29, 4875–4894. 2019. https://doi.org/10.1108/HFF-04-2019-0277

[15] Grosan, T.; Pop, I, "Forced convection boundary layer flow past non-isothermal thin needles in nanofluids",J. Heat Transf., 133, 054503, 2011. https://doi.org/10.1115/1.4003059

[16] Soid, S.K.; Ishak, A.; Pop, I., "Boundary layer flow past a continuously moving thin needlein a nanofluid". Appl. Therm. Eng., 114, 58–64,2017. https://doi.org/10.1016/j.applthermaleng.2016.11.165

[17] G.G. Momin, "Experimental investigation of mixed convection with water-Al2O3 & hybrid nanofluid in inclined tube for laminar flow", Int. J. Sci. Technol. Res., 2,195–202, 2013. http://citeseerx.ist.psu.edu/viewdoc/download?doi=10.1.1.588.5334&rep=rep1&type=pdf

[18] Ahmad, S.; Arifin, N.M.; Nazar, R.; Pop, I. "Mixed convection boundary layer flow along vertical thin needles Assisting and opposing flows", Int. Commun. Heat Mass Transf., 35, 157–162,2008. https://doi.org/10.1016/j.icheatmasstransfer.2007.07.005

[19] Trimbitas, R., Grosan, T. and Pop, I "Mixed convection boundary layer flow along vertical thin needles in nanofluids", International Journal of Numerical Methods for Heat & Fluid Flow, 24, 579-594, 2014. https://doi.org/10.1108/HFF-05-2012-0098

[20] A. J. Chamkha, "Solar Radiation Assisted Natural Convection in Uniform Porous Medium Supported by a Vertical Flat Plate", Heat Transfer. , 119(1), 89-96, 1997. https://doi.org/10.1115/1.2824104

[21] A.J Chamkha, Camille. I. "Natural convection from an inclined plate embedded in a variable porosity porous medium due to solar radiation." International Journal of Thermal Sciences, 41,73-81, 2002. https://doi.org/10.1016/S1290-0729(01)01305-9 .

[22] Aamir Hamid, "Terrific effects of Ohmic-viscous dissipation on Casson nanofluid flow over a vertical thin needle: buoyancy assisting & opposing flow", Journal of Materials Research and Technology,9, 11220-11230, 2020. https://doi.org/10.1016/j.jmrt.2020.07.070

[23] Waini, I.; Ishak, A.; Pop, I, "Hybrid Nanofluid Flow Past a Permeable Moving Thin Needle", Mathematics,8, 2020. https://doi.org/10.3390/math8040612

[24] W.A. Khan & A. Aziz, "Natural convection flow of a nanofluid over a vertical plate with uniform surface heat flux", International Journal of Thermal Sciences, 50,1207-1214, 2011. https://doi.org/10.1016/j.ijthermalsci.2011.02.015

[25] O.D. Makinde & A. Aziz, "Boundary layer flow of a nanofluid past a stretching sheet with a convective boundary condition", International Journal of Thermal Sciences, 50, 1326-1332, 2011. https://doi.org/10.1016/j.ijthermalsci.2011.02.019